Mitigation of Intercore Crosstalk Impact over Multi-band MCF Transmission using Bandwidth-partitioned Spectral Inversion

Megumi Hoshi(1), Kohki Shibahara(1), Shimpei Shimizu(1), Takayuki Kobayashi(1), Masanori Nakamura(1), Takushi Kazama(1,2), Takeshi Umeki(1,2), Takayoshi Mori(3), Yusuke Yamada(3), Kazuhide Nakajima(3), Yutaka Miyamoto(1)

(1) NTT Network Innovation Laboratories, NTT Corporation, megumi.hoshi@ntt.com
(2) NTT Device Technology Laboratories, NTT Corporation
(3) NTT Access Network Service Systems Laboratories, NTT Corporation

Abstract *We propose a bandwidth-partitioned spectral inversion (BPSI) technique to mitigate intercore-crosstalk impact over multi-band MCF transmission. A decreased wavelength-dependent crosstalk difference was experimentally achieved over four-core MCF below 1 dB even using C+L band by PPLN-based BPSI, negligible OSNR-penalty variation in 96-Gbaud PCS64QAM signal transmission. ©2023 The Author(s)*

Introduction

To overcome the growing capacity demand for optical transmission systems, the combination of multi-band transmission [1,2] and space-division multiplexing technologies [3] is promising. Each technique has several effects on wavelength or space channels, such as stimulated Raman scattering [4,5] and non-linear interference noise [5], and when using a weakly-coupled multicore fibre (MCF) system, intercore crosstalk (IXT) is one factor to be considered [6]. When aiming to achieve multi-band MCF transmission [7], the wavelength-dependence of IXT becomes a major issue [8,9]. IXT increases linearly in units of dB with the wavelength [10,11], resulting in a 10 dB-IXT difference over the C+L band, which makes the system design more complicated when the other effects mentioned above are included. Thus, to mitigate this complexity, IXT-flattening mechanisms used over multi-band transmission are desired.

We previously proposed a spectral-inversion (SI) technique that decreases the slope of the IXT spectrum and demonstrated it by simultaneously "flipping" the optical spectrum through PPLN-based optical phase conjugation [12]. In this paper, we extend the SI technique to support multi-band MCF transmission covering the entire C+L band with further decreased IXT variation, referred to as bandwidth-partitioned spectral inversion (BPSI). Experimental validation results over four-core MCF show a decreased IXT difference of less than 1 dB over the C+L band, a flattened OSNR penalty and generalized mutual information (GMI) for each wavelength channel.

Proposed method: Bandwidth-partitioned spectral inversion

This section presents BPSI and the calculations on which it is based. Figure 1(a) shows a schematic diagram of the system for applying the conventional SI technique [12]. The transmission line is divided into several spans, and signals are spectrally inverted at each node. The transmission signals which experience IXT from

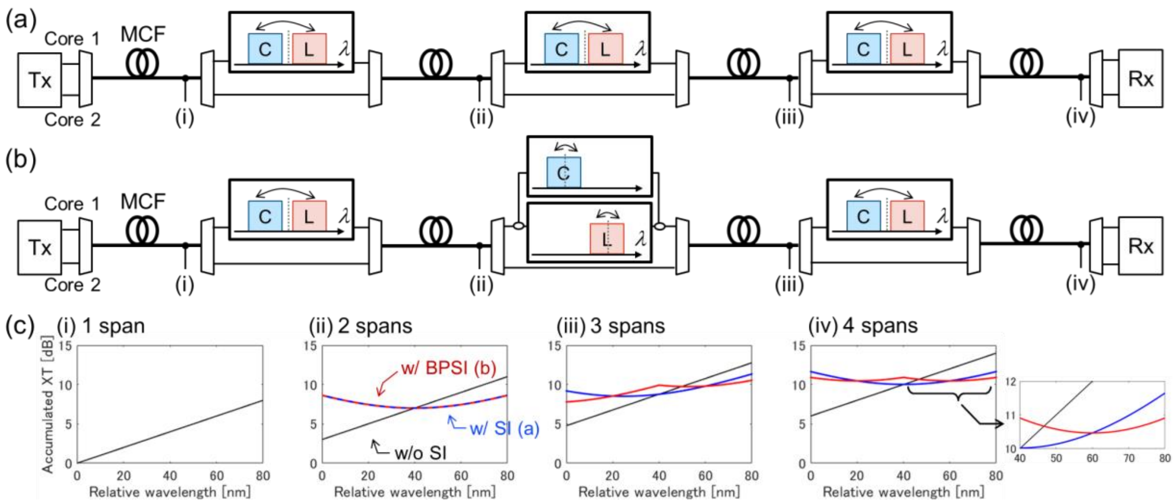

Fig. 1: Transmission system example over 2-core fiber including optical nodes with (a) SI [12] and (b) BPSI, in which SIs are applied to one core. (c) Schematic spectra of accumulated IXT from each span.

the longer-wavelength side at the i-th span are inverted to the shorter-wavelength side and vice versa; then, the spectrum of accumulated IXT is flattened over the wavelength. In the case of multi-band transmission, however, this method leaves a relatively large IXT slope, as shown in the convex-down graph in Fig. 1(c)-(ii). BPSI is proposed to decrease this remaining slope, by adding narrow-bandwidth SIs with multiple centre wavelengths. Figure 1(b) shows a schematic diagram assuming a C+L multi-band system whose bandwidth is 80 nm (10 THz) in summation. In this example, the transmission line is divided into four spans, and signals are inverted at the nodes, and the centre wavelengths of each inversion are different. Three centre wavelengths of inversion are set: (i) between the C-band and L-band, (ii) at the centre of the C-band and (iii) at the centre of the L-band. Combining these inverters and allocating them at appropriate points, it is possible to flatten the IXT spectrum as compared with the conventional SI method, shown in Fig. 1(c). Thus, the BPSI provides uniform transmission performance over the C+L band.

IXT-induced SNR penalty on achievable transmission capacity with/without SI

In this section, we clarify the achievable capacity based on the IXT-affected SNR, which we will refer to as $\mathrm{SNR_{eff}}$, before/after applying the SI technique.

In the presence of IXT, $\mathrm{SNR_{eff}}$ is written as:

$$\mathrm{SNR_{eff}} = \left(\mathrm{SNR_0}^{-1} + N\ \mathrm{IXT}(\lambda_i)\right)^{-1} \qquad (1)$$

where $\mathrm{SNR_0}$ is defined as P_{sig} / P_{ASE} (P_{sig}: signal power, P_{ASE}: ASE noise power), N as the number of spans, $\mathrm{IXT}(\lambda_i)$ as the IXT ratio per span P_{XT} / P_{sig}, and i as the wavelength channel number. When using the IXT flattening technique including SI or BPSI, the IXT variation range becomes narrower, and in an ideal case, in which the IXT spectrum becomes completely flat, the IXT over the bandwidth of interest has one value, $\mathrm{IXT_{flat}} = N\ \Sigma_{i=1}^{n}\ \mathrm{IXT}(\lambda_i)/n$. Fig. 2(a) shows the comparison of distance-independent [9] SNR penalty (= $\mathrm{SNR_0}$ / $\mathrm{SNR_{eff}}$) induced by IXT with and without IXT flattening, assuming the wavelength and IXT axes in Fig. 1(c)-(iv) for step-index or trench-assisted fibre transmission, set to IXT = –40 dB or –60 dB at 1550 nm [13] and IXT slope to 0.1 dB/nm [11]. Both types of MCFs are capable of long-haul transmission [9,14], and the SI or BPSI makes it possible to reduce the impact of IXT-induced SNR penalty over the C+L band, as well as to utilize longer-wavelength resources which was affected by large IXT. Its effect is more dominant with large-IXT MCF.

Comparing the capacity for each of these cases, with $C_{\mathrm{w/o\ SI}}$ as the case without SI and C_{flat} as the case in which the IXT spectrum is completely flattened, they follow Jensen's inequality below:

$$\begin{aligned}
C_{\mathrm{w/o\ SI}} &= \Sigma_{i=1}^{n} B\log_2(1+\mathrm{SNR_{eff,w/oSI}}) \\
&= \Sigma_{i=1}^{n} B\log_2\left[1+\left(\mathrm{SNR_0}^{-1}+N\mathrm{IXT}(\lambda_i)\right)^{-1}\right] \\
&\cong -\Sigma_{i=1}^{n} B\log_2\left(\mathrm{SNR_0}^{-1}+N\mathrm{IXT}(\lambda_i)\right) \\
&> -nB\log_2\left(\mathrm{SNR_0}^{-1}+N\frac{\Sigma_{i=1}^{n}\mathrm{IXT}(\lambda_i)}{n}\right) \\
&= -nB\log_2\left(\mathrm{SNR_0}^{-1}+N\mathrm{IXT_{flat}}\right) \triangleq C_{\mathrm{flat}} \qquad (2)
\end{aligned}$$

where B is the bandwidth occupied by a modulated signal. Based on the inequality above, the total capacity slightly decreases when the IXT spectrum becomes flat. Figure 2(b) shows the decreased capacity ratio with IXT-flattening, C_{flat} / $C_{\mathrm{w/o\ SI}}$, in step-index MCF transmission assumed, $\mathrm{SNR_0}$ set to 25–35 dB. The capacity decreases more with IXT flattening as the bandwidth expands and $\mathrm{SNR_0}$ is higher, by 1% within the C+L band under $\mathrm{SNR_0}$ = 35 dB. This should be a slight difference and negligible, but there found to be a trade-off relationship between IXT flatness and capacity; thus, pros and cons have to be considered in optimizing transmission systems.

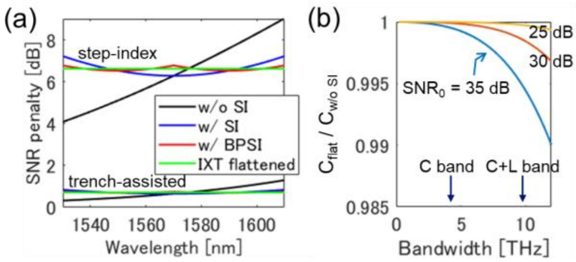

Fig. 2: (a) SNR penalties with/without SI or BPSI.
(b) Ratio of C_{flat} and $C_{\mathrm{w/o\ SI}}$ for each bandwidth for step-index MCF transmission.

Experimental setup

We ran two experiments on BPSI: (i) IXT spectrum measurement and (ii) signal transmission under the effect of IXT. Fig. 3 shows the experimental setup. 5-km step-index 4-core MCF [15] was used as one span of transmission line. The transmission loss of this MCF was 0.19 dB/km, and IXT was –40 dB/km (at 1550 nm) for each core. For BPSI, optical phase conjugation using a PPLN-based optical parametric amplifier (OPA) was applied, whose centre wavelength for inversion was set to λ_{C} = 1545.23 nm (= 194.0 THz) [16] and λ_{CL} = 1572.89 nm (= 190.6 THz) [17]. The amplification gain of the OPA with SI was set to compensate for the loss of each span, combined with optical equalisers. The IXT source was generated over the C+L band with equalized ASE light over 1529.55–1618.75 nm. Core #1 in Fig. 3 was used as the transmission line, and the neighbouring cores (#2 and #4) were used to load

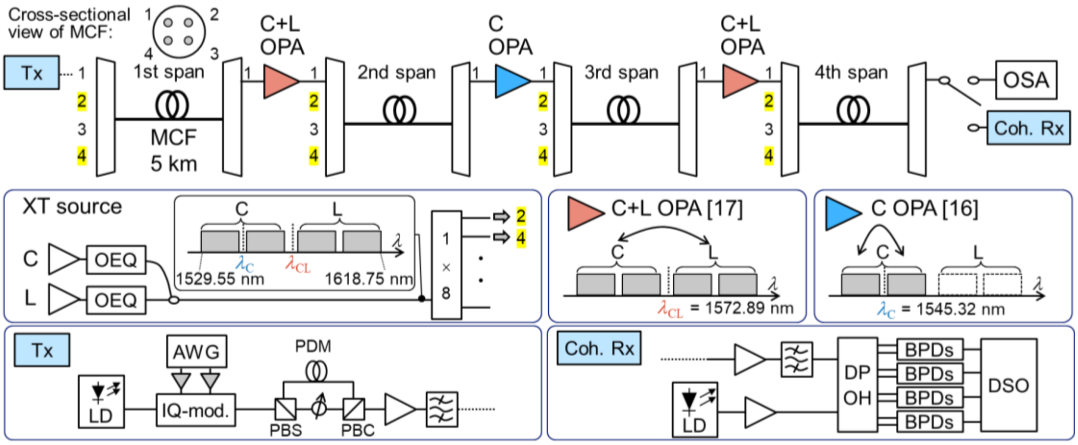

Fig. 3: Experimental setup for BPSI demonstration. OSA: optical spectrum analyzer, OEQ: optical equalizer, AWG: arbitrary waveform generator, PBS/PBC: polarization beam splitter/combiner, DPOH: dual polarization optical hybrid, BPD: balanced photodetector, DSO: digital storage oscilloscope.

the IXT source, which was split into the 8 fibres highlighted in yellow, in order to load the same IXT source power in each span.

(i) Accumulated IXT spectra were obtained from the output of the 4th span by an optical spectrum analyser. (ii) A Nyquist-pulse-shaped 96-Gbaud PCS64QAM signal with a 0.03-roll-off factor in the C- or L-band [18] passed through a polarisation-multiplexing emulator and was loaded to the transmission line (core #1). The entropy of the PCS64QAM was 5.285 bit/2D symbol. The signal at each wavelength was transmitted through 4 spans and was received by a coherent receiver. Afterwards, the signal was recovered by digital signal processing algorithms including chromatic dispersion compensation, MIMO equalization, and carrier phase recovery with 1.64% periodically inserted pilot symbols [18]. Bit-wise log-likelihood ratios (LLRs) were calculated by bit-metric decoding, and the GMIs for PCS-64QAM were computed with the LLRs.

Results

Fig. 4(a) shows that the accumulated IXT spectrum had a slope larger than 0.1 dB/nm and ΔIXT_{pp} > 8 dB over the C+L band, shown by the black dots. With conventional SI [12], in which the signal was inverted at λ_{CL} = 1572.89 nm, only the point between the 2nd and the 3rd span had decreased slopes of 0.063 or 0.070 dB/nm and ΔIXT_{pp} of 3 dB. With the proposed BPSI method, the IXT slope was reduced to 0.014 or 0.022 dB/nm and ΔIXT_{pp} to less than 1 dB. With BPSI, only the accumulated IXT spectra of the L-band were obtained because of a limitation of the experimental setup. Fig. 4(b) shows the OSNR penalty for the signal at each wavelength. These penalties were obtained by the OSNR difference between the case with and without IXT loading. As compared to the case without SI, the OSNR penalty showed a decreased slope with BPSI,

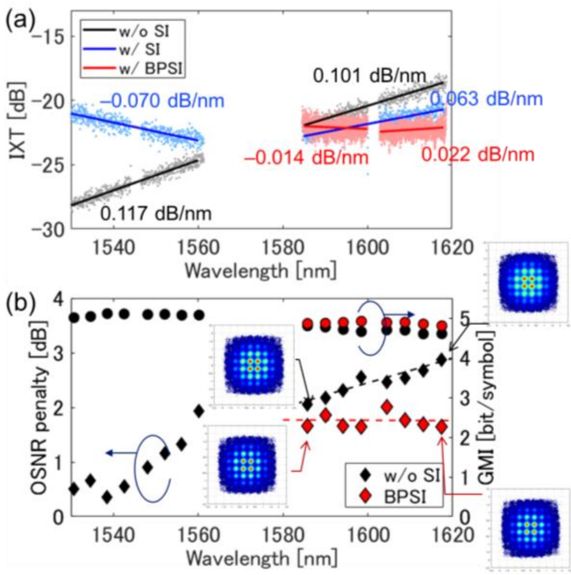

Fig. 4: (a) Spectra of accumulated IXT, without SI, with SI applied, with BPSI applied. (b) OSNR penalties and GMI (per polarization) of each wavelength channel. Black: w/o SI, red: w/ BPSI.

and its difference was less than 0.5 dB. As for the capacity, the average achievable throughput calculated from GMI was 937.2 bps/λ in the case without SI and 934.8 bps/λ with BPSI, showing 0.3% of slight and negligible capacity decrease.

Conclusion

We proposed the BPSI method, which decreases the wavelength dependence of IXT over multi-band transmission. With PPLN-based BPSI, we experimentally demonstrated that this method mitigated the IXT difference over the C+L band to less than 1 dB and achieved 96-Gbaud PCS64QAM transmission with less OSNR variety for each wavelength channel.

Acknowledgements

Part of this research is supported by NICT, Japan under commissioned research No. 20301.

References

[1] F. Hamaoka, K. Saito, A. Masuda, H. Taniguchi, T. Sasai, M. Nakamura, T. Kobayashi and Y. Kisaka, “112.8-Tb/s real-time transmission over 101 km in 16.95-THz triple-band (S, C, and L bands) WDM configuration,” presented at *OptoElectronics and Communications Conference*, Toyama, Japan, 2022, PDP-A-3. DOI: 10.23919/OECC/PSC53152.2022.9849881

[2] T. Kato, H. Irie, H. Muranaka, Y. Tanaka, Y. Akiyama and T. Hoshida, “U-band transmission of real-time 200-Gb/s signal co-propagating with C+L-band WDM signal,” presented at *Optical Fiber Communications Conference and Exhibition*, San Diego, USA, 2023, Th3F.3

[3] T. Mizuno, H. Takara, K. Shibahara, A. Sano and Y. Miyamoto, “Dense space division multiplexed transmission over multicore and multimode fiber for long-haul transport systems,” *Journal of Lightwave Technology*, vol. 34, no. 6, pp. 1484–1493, 2016. DOI: 10.1109/JLT.2016.2524546

[4] G. Rademacher, R. S. Luis, B. J. Puttnam, Y. Awaji and M. Wada, “Experimental investigation of stimulated Raman scattering induced crosstalk-tilt in a homogeneous multi-core fiber”, presented at *Asia Communications and Photonics. Conference*, Chengdu, China, 2009, S3A.

[5] D. Semrau, R. I. Kelley, and P. Bayvel, “A closed-form approximation of the Gaussian noise model in the presence of inter-channel stimulated Raman scattering,” *Journal of Lightwave Technology*, vol. 37, no. 9, pp. 1924–1936, 2019. DOI: 10.1109/JLT.2023.3256185

[6] T. Hayashi, T. Taru, O. Shimakawa, T. Sasaki, and E. Sasaoka, “Uncoupled multi-core fiber enhancing signal-to-noise ratio,” *Optics Express*, vol. 20, no. 26, pp. B94-B103, 2012. DOI: 10.1364/OE.20.000B94

[7] B. J. Puttnam et al., “319 Tb/s transmission over 3001 km with S, C, and L band signals over >120 nm bandwidth in 125 μm wide 4-core fiber,” presented at *Optical Fiber Communications Conference and Exhibition*, San Francisco, USA, 2021, F3B.3. DOI: 10.1364/OFC.2021.F3B.3

[8] B. J. Puttnam et al., “Inter-core crosstalk penalties in wideband WDM, MCF transmission over transoceanic distances,” presented at *European Conference on Optical Communication*, Rome, Italy, 2018, Th1J.1. DOI: 10.1109/ECOC.2018.8535348

[9] R. S. Luis, G. Rademacher, B. J. Puttnam, D. Semrau, R. I. Killey, P. Bayvel, Y. Awaji and H. Furukawa, “Crosstalk impact in the performance of wideband multicore-fiber transmission systems”, *IEEE Journal of selected topics in quantum electronics*, vol. 26, no. 4, pp. 1244–1245, 2020. DOI: 10.1109/JSTQE.2020.2975662

[10] B. Li et al., “Investigation on the wavelength dependent crosstalk of multicore fibers,” presented at *Optical Fiber Communications Conference and Exhibition*, Anaheim, USA, 2013, AF1D.5. DOI: 10.1364/ACPC.2013.AF1D.5

[11] F. Ye et al., “Wavelength-dependence of inter-core crosstalk in homogeneous multi-core fibers,” *IEEE Photonics Technology Letters*, vol. 28, no. 1, pp. 27–29, 2016. DOI: 10.1109/LPT.2015.2478911

[12] M. Hoshi, K. Shibahara, S. Shimizu, T. Kobayashi, T. Umeki, T. Kazama, K. Watanabe, T. Mori, Y. Yamada, K. Nakajima and Y. Miyamoto, “Mitigation of Intercore Crosstalk Impact by PPLN-based Optical Spectrum Inversion”, presented at *OptoElectronics and Communications Conference*, Toyama, Japan, 2022, TuB2-3. DOI: 10.23919/OECC/PSC53152.2022.9849942

[13] K. Saitoh and S. Matsuo, “Multicore fiber technology,” *Journal of Lightwave Technology*, vol. 34, no. 1, pp. 55–66, 2016, DOI: 10.1109/JLT.2015.2466444

[14] K. Shibahara, M. Hoshi, T. Matsui, T. Mori, K. Nakajima and Y. Miyamoto, “Long-haul unidirectional transmission over weakly-coupled MCF with distance-insensitive inter-core skew spread,” presented at *Optical Fiber Communications Conference and Exhibition*, San Diego, USA, 2023, M2B.5.

[15] T. Matsui, Y. Yamada, Y. Sagae and K. Nakajima, “Standard cladding diameter multi-core fiber technology,” presented at *Optical Fiber Communications Conference and Exhibition*, San Diego, USA, 2021, Tu6B.4, DOI: 10.1364/OFC.2021.Tu6B.4

[16] T. Umeki et al., “Simultaneous nonlinearity mitigation in 92 × 180-Gbit/s PDM-16QAM transmission over 3840 km using PPLN-based guard-band-less optical phase conjugation”, *Optics Express*, vol. 24, issue 15, pp. 16945–16951, July 2016. DOI: 10.1364/OE.24.016945

[17] S. Shimizu, T. Kobayashi, A. Kawai, T. Kazama, M. Nakamura, K. Enbutsu, T. Kashiwazaki, M. Abe, T. Umeki, Y. Miyamoto, T. Kato, Y. Tanaka and T. Hoshida, “38.4-Tbps Inline-amplified Transmission Using PPLN-based Optical Parametric Amplifier over 6 THz within L- and U-bands”, presented at *Optical Fiber Communications Conference and Exhibition*, San Diego, USA, 2023, Th3F.3.

[18] T. Kobayashi, M. Nakamura, F. Hamaoka, M. Nagatani, H. Wakita, H. Yamazaki, T. Umeki, H. Nosaka and Y. Miyamoto, ”35-Tb/s C-Band Transmission Over 800 km Employing 1-Tb/s PS-64QAM Signals Enhanced by Complex 8 × 2 MIMO Equalizer”, presented at *Optical Fiber Communications Conference and Exhibition*, 2019, USA, PDP. Th4B.2, DOI: 10.1364/OFC.2019.Th4B.2